cAMP Regulated Membrane Diffusion of a Green Fluorescent Protein-Aquaporin 2 Chimera

Fuminori Umenishi,* Jean-Marc Verbavatz,† and A. S. Verkman*

*Departments of Medicine and Physiology, Cardiovascular Research Institute, University of California, San Francisco, California 94143-0521, USA, and †Service de Biologie Cellulaire, Commissariat à l'Energie Atomique/Saclay, F-91191 Gif-sur-Yvette, France

ABSTRACT To study the membrane mobility of aquaporin water channels, clones of stably transfected LLC-PK1 cells were isolated with plasma membrane expression of GFP-AQP1 and GFP-AQP2, in which the green fluorescent protein (GFP) was fused upstream and in-frame to each aquaporin (AQP). The GFP fusion did not affect AQP tetrameric association or water transport function. GFP-AQP lateral mobility was measured by irreversibly bleaching a spot (diameter 0.8 μm) on the membrane with an Argon laser beam (488 nm) and following the fluorescence recovery into the bleached area resulting from GFP translational diffusion. In cells expressing GFP-AQP1, fluorescence recovered to >96% of its initial level with $t_{1/2}$ of 38 ± 2 s (23°C) and 21 ± 1 s (37°C), giving diffusion coefficients (D) of 5.3 and 9.3 × 10^{-11} cm^2/s. GFP-AQP1 diffusion was abolished by paraformaldehyde fixation, slowed >50-fold by the cholesterol-binding agent filipin, but not affected by cAMP agonists. In cells expressing GFP-AQP2, fluorescence recovered to >98% with D of 5.7 and 9.0 × 10^{-11} cm^2/s at 23°C and 37°C. In contrast to results for GFP-AQP1, the cAMP agonist forskolin slowed GFP-AQP2 mobility by up to tenfold. The cAMP slowing was blocked by actin filament disruption with cytochalasin D, by K^+-depletion in combination with hypotonic shock, and by mutation of the protein kinase A phosphorylation consensus site (S256A) at the AQP2 C-terminus. These results indicate unregulated diffusion of AQP1 in membranes, but regulated AQP2 diffusion that was dependent on phosphorylation at serine 256, and an intact actin cytoskeleton and clathrin coated pit. The cAMP-induced immobilization of phosphorylated AQP2 provides evidence for AQP2-protein interactions that may be important for retention of AQP2 in specialized membrane domains for efficient membrane recycling.

INTRODUCTION

The aquaporin water channels comprise a family of homologous proteins that number ten in mammals, with many more in plants and lower organisms (reviewed in Verkman et al., 1996; Lee et al., 1997; Deen and van Os, 1998). The most studied protein, aquaporin-1 (AQP1), is a 28-kDa glycoprotein that forms tetramers in membranes (Smith and Agre, 1991; Verbavatz et al., 1993) in which the monomers function independently (Shi et al., 1994). Each AQP1 monomer consists of six tilted helical segments that span the membrane and surround a putative aqueous pore (Cheng et al., 1997; Walz et al., 1997). AQP1 protein is expressed in erythrocytes, kidney tubules, and various epithelia and endothelia, where it appears to be constitutively functional and localized at the plasma membrane. Recent studies of transgenic AQP1 null mice implicate an important physiological role for AQP1 in the urinary concentrating mechanism (Ma et al., 1998) and lung fluid transport (Bai et al., 1999).

In contrast to AQP1, aquaporin-2 (AQP2) is a regulated water channel expressed in kidney collecting-duct epithelial cells (reviewed in Knepper and Inoue, 1997; Yamamoto and Sasaki, 1998; Nielsen et al., 1999). Mutations in AQP2 cause hereditary nephrogenic diabetes insipidus (Deen et al., 1994) in which misfolded mutant AQP2 is retained at the endoplasmic reticulum resulting in low collecting-duct water permeability and excretion of hypotonic urine (Deen et al., 1995; Bichet, 1998; Tamarappoo and Verkman, 1998; Tamarappoo et al., 1999). Transcellular water permeability in collecting duct is regulated by a membrane-cycling mechanism, where vesicles containing functional AQP2 water channels are inserted into and retrieved from the apical plasma membrane in response to the antidiuretic hormone vasopressin. The insertion of AQP2-containing vesicles into the plasma membrane appears to require phosphorylation of residue serine 256 at the AQP2 C-terminus (Fushimi et al., 1997; Katsura et al., 1997). Unique characteristics of the AQP2 membrane-cycling mechanism include continued exocytosis and endocytosis during vasopressin stimulation (Verkman et al., 1988; Katsura et al., 1995), and targeting of internalized AQP2 to a nonacidic endosomal compartment (Lencer et al., 1990). The AQP2-containing vesicles appear to coexpress various molecules involved in membrane trafficking, including synaptobrevin-2 (VAMP-2) (Nielsen et al., 1995b), syntaxin-4 (Mandon et al., 1996), SNAP-23 (Inoue et al., 1998), and dynein and dynactin (Marples et al., 1998), although there is no direct proof that these molecules are involved in AQP2 trafficking. There is evidence that actin is involved in AQP2 trafficking (Brown et al., 1996) and that AQP2 endocytosis is mediated by clathrin-coated vesicles (Strange et al., 1988), but there has been no direct demonstration of interactions between AQP2 and other proteins. Recently, transfected epithelial cell culture models have been generated that recapitulate cAMP-

Received for publication 23 June 1999 and in final form 27 October 1999.

Address reprint requests to Alan S. Verkman, 1246 Health Sciences East Tower, Cardiovascular Research Institute, University of California–San Francisco, San Francisco, CA 94143-0521. Tel.: 415-476-8530; Fax: 415-665-3847; E-mail: verkman@itsa.ucsf.edu.

0006-3495/00/02/1024/12 $2.00

regulated AQP2 membrane trafficking (Katsura et al., 1995; Valenti et al., 1996; Deen et al., 1997; Fushimi et al., 1997), including cells expressing a GFP-AQP2 chimera (Gustafson et al., 1998).

As suggested recently for cystic fibrosis transmembrane regulator (CFTR) (Kornau et al., 1997), glucose transporter (GLUT-4) (James et al., 1994) and other membrane proteins, regulated protein trafficking and/or transport activity involves protein–protein interactions. We report here the application of a biophysical approach to test whether cAMP-regulation of AQP2 involves interaction between AQP2 and other proteins at the plasma membrane. Fluorescence recovery after photobleaching (FRAP) was used to quantify the membrane diffusion of GFP-aquaporin chimeras in transfected cells. It was found that the mobility of GFP-AQP1 at the plasma membrane was unregulated, whereas the mobility of GFP-AQP2 was remarkably reduced by cAMP agonists in a manner that was dependent on AQP2 phosphorylation, and an intact actin cytoskeleton and clathrin-coated pit. The reduced AQP2 mobility after phosphorylation provides direct biophysical evidence for interaction of plasma membrane AQP2 with as yet undefined regulatory protein(s).

MATERIALS AND METHODS

cDNA constructs and cell transfection

The cDNAs encoding GFP-AQP1 and GFP-AQP2 were prepared by subcloning the cDNA coding sequence of rat AQP1 and AQP2 in frame into *Bam*H I/*Xba* I and *Bgl* II/*Xba* I sites of plasmid pEGFP-C1 (Clonetech Laboratories, Inc., Palo Alto, CA). The point mutation S256A was generated by polymerase chain reaction. The AQP2-S256A cDNA was subcloned into the *Bgl* II/*Xba* I site of pEGFP-C1, and the mutation was confirmed by sequence analysis.

LLC-PK1 (ATCC CL-101) and MDCK (ATCC CCL-34.2) renal epithelial cells were obtained from the American Type Culture Collection and cultured at 37°C in 5% CO_2 in Dulbecco's modified eagle medium (DMEM) supplemented with 10% fetal bovine serum. Cell transfection was performed by electroporation as described previously (Umenishi and Verkman, 1998). Briefly, LLC-PK1 and MDCK cells were suspended at 10^7 cells/ml in DMEM without serum and transfected in an electroporator (Invitrogen, San Diego, CA) set at 1000 μF and 330 V. Transfection was done with 20 μg of GFP-AQP1 or GFP-AQP2 cDNA in a total volume of 250 μl. After 48 h incubation, transfected cells were selected and maintained in medium containing Geneticin (G418; GIBCO, Grand Island, NY) for two weeks. The resultant clones were isolated and used for further analysis.

Water permeability measurements

Rat AQP1, AQP2, GFP-AQP1 and GFP-AQP2 cDNAs were subcloned into oocyte expression plasmid pSP65T (Zhang et al., 1993). cRNA was synthesized using SP6 RNA polymerase and 2 μg of linearized plasmid DNA in the presence of diguanosine triphosphate (Pharmacia Biotech., Piscataway, NJ). After DNase digestion, cRNA was purified by phenol-chloroform extraction and ethanol precipitation.

Stage V and VI oocytes from *Xenopus laevis* were isolated, defolliculated and microinjected with 50 nl water or cRNA samples (10 ng/μl). Oocytes were incubated at 18°C for 24 h and osmotic water permeability (P_f) was measured from the time course of oocyte swelling at 10°C in response to a fivefold dilution of the extracellular Barth's buffer with distilled water.

Immunoblot analysis

Cells grown on a 10-cm dish were rinsed with PBS and scraped off with 1 ml of homogenization buffer (10 mM Tris, 200 mM sucrose, 1 mM EDTA, 1 mM PMSF, 1 μg/ml pepstatin A, 1 μg/ml aprotinin, pH 7.4). The homogenate was centrifuged at 2,000 g for 10 min, and the supernatant was spun at 14,000 g for 10 min. The membrane was pelleted at 100,000 g for 60 min, and solubilized in Laemmli sample buffer. Membrane proteins were resolved on a 10% SDS-polyacrylamide gel and transferred to a PVDF membrane. The membrane was incubated with polyclonal antibodies against GFP, AQP1 or AQP2, and a secondary anti-rabbit IgG horseradish peroxidase antibody. Detection was done enhanced chemiluminescence (Boehringer Mannheim, Indianapolis, IN).

Freeze-fracture electron microscopy

Cells expressing GFP-AQP1 and GFP-AQP2 were grown to confluence on plastic plates, fixed for 1 h in 2% glutaraldehyde in PBS, and washed in phosphate buffered saline (PBS). Cells were scraped, infiltrated in 30% glycerol for 30 min and frozen in liquid N_2-cooled Freon. Freeze-fracture was carried out as described previously (Verbavatz et al., 1997). Briefly, samples were fractured at -150°C under a 10^{-7} Torr vacuum and shadowed with platinum at 45°, followed by carbon at 90°. The platinum/carbon replicas were washed in bleach and water, and examined by electron microscopy. Intramembrane particle (IMP) densities were quantified on P-face freeze-fracture micrographs of the basolateral plasma membrane at 80,000× magnification from >6 different cells with total surface area >0.3 μm^2. IMP diameters were measured on photographs at 320,000x final magnification. More than 300 IMPs were measured for each condition and IMP density versus IMP diameter data were fitted to Gaussian distributions by nonlinear least-squares regression.

Fluorescence recovery after photobleaching

Cells were grown on 18-mm-diameter round glass coverslips until near confluence and the coverslip was mounted in a perfusion chamber. FRAP measurements were carried out on an apparatus described previously (Kao and Verkman, 1996). An Argon ion laser beam (488 nm, Innova 70–4; Coherent Inc., Palo Alto, CA) was modulated by an acousto-opic modulator (1.5 μs response time) and directed onto the stage of an inverted epifluorescence microscope (Diaphot; Nikon Inc., Melville, NY). The microscope was also equipped for full-field epi-illumination to visualize all cells to target the focused laser beam. The full-field and laser beams were reflected by a dichroic mirror (510 nm) onto the sample by a 100× objective lens (Nikon Fluor, numerical aperture 1.4). For most experiments, the laser beam power was set to 200–500 mW (488 nm) and the attenuation ratio (the ratio of bleach to probe beam intensity) was 5000–15000. Sample fluorescence was filtered by serial barrier (Schott glass OG 515) and interference (530 ± 15 nm) filters and detected with a photomultiplier, transimpedence amplifier and 12-bit analog-to-digital converter. A gating circuit that controls the voltage of the second dynode was used to decrease photomultiplier gain during photobleaching. An electronic shutter was used in the excitation path to illuminate the sample intermittently during the probe period to avoid photobleaching by the probe beam. Signals were sampled before the bleach and at 1–2-s intervals (25-ms

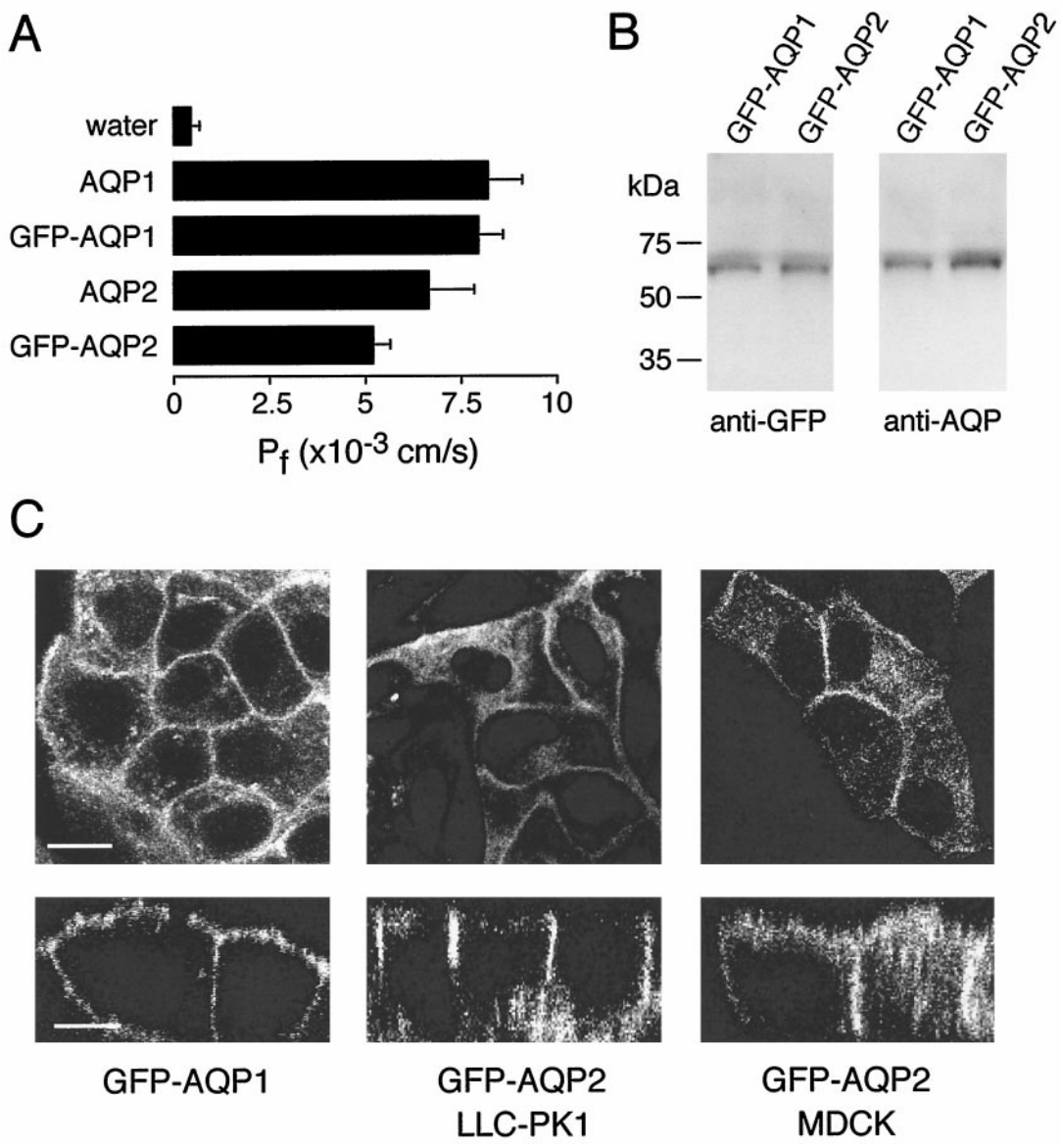

FIGURE 1 Functional analysis and localization of GFP-aquaporins. (A) Water permeability in *Xenopus* oocytes microinjected with water or 5 ng cRNA encoding indicated aquaporins. Measurements were done at 10°C using the established swelling assay (see Methods). (*B*) Immunoblot analysis of microsomal membranes from GFP-AQP1 and GFP-AQP2 expressing LLK-PK1 cells using indicated anti-GFP or anti-aquaporin polyclonal antibodies. (*C*) Laser scanning confocal microscopy of transfected GFP-AQP1 and GFP-AQP2 in LLC-PK1 cells (*left* and *middle panels*), and GFP-AQP2 in MDCK cells (*right panels*). The micrographs include *xy* (*top*) and *xz* (*bottom*) reconstructions. Scale bar: 10 μm.

sampling time) after the bleach. Unless otherwise specified, measurements were done at 23°C in a temperature-controlled darkroom.

Analysis of FRAP data

Recovery half-time ($t_{1/2}$), defined as the time when fluorescence recovered by 50%, was determined from fluorescence recovery curves, $F(t)$, as described by Swaminathan et al. (1996). Apparent diffusion coefficients (D, cm^2/s) were computed from $t_{1/2}$ using information about beam spot size (0.8-μm-diameter spot for 100× lens) and bleach geometry. Because the cell edge was targeted by the laser beam in the bleaching studies, it was assumed that the bleached zone consisted of a rectangular strip of membrane oriented parallel to the beam axis. Recovery into the bleached zone was then described by the diffusion equation in one-dimension (Partikian et al., 1998), whose solution predicts,

$$F(t) = F_0\left[1 - \frac{f_b}{2d}\int_{-d/2}^{d/2}\left\{\mathrm{erf}\left(\frac{d/2 - x}{2(Dt)^{1/2}}\right) + \mathrm{erf}\left(\frac{d/2 + x}{2(Dt)^{1/2}}\right)\right\}\mathrm{d}x\right], \quad (1)$$

where d is beam diameter, F_0 is the prebleach fluorescence, f_b is the fractional bleach, and erf(x) is the error function. D values were computed

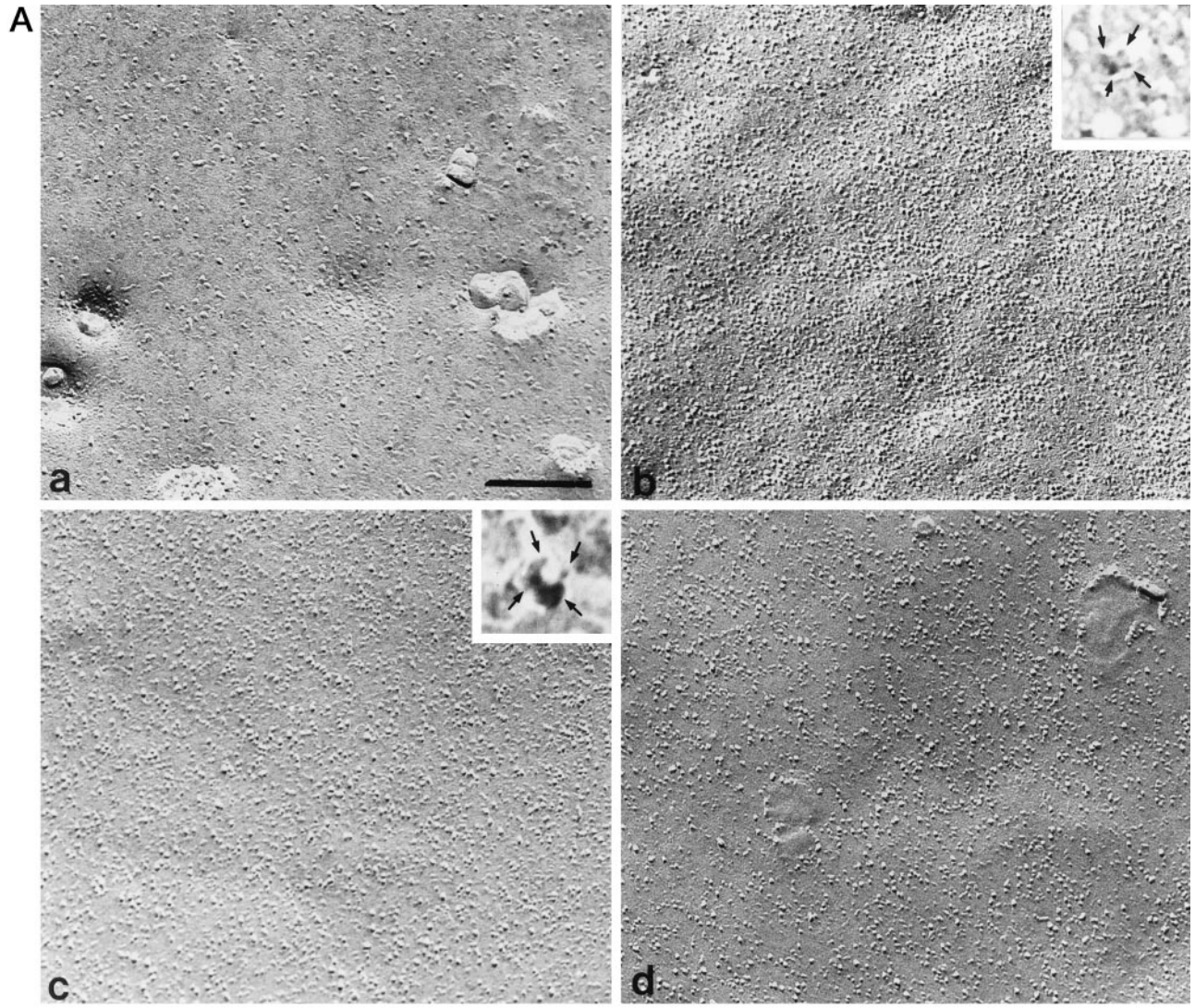

FIGURE 2 Freeze-fracture electron microscopy of basolateral plasma membranes of GFP-aquaporin-expressing LLC-PK1 cells. (*A*) Control LLC-PK1 cells (*panel a*) and LLC-PK1 expressing GFP-AQP1 (*panel b*), and GFP-AQP2 before (*panel c*) and after (*panel d*) forskolin stimulation. Scale bar, 200 nm. At high magnification, IMP tetramers, typical of aquaporins, were observed for both GFP-AQP1 (*panel b*, *inset*) and GFP-AQP2 (*panel c*, *inset*)

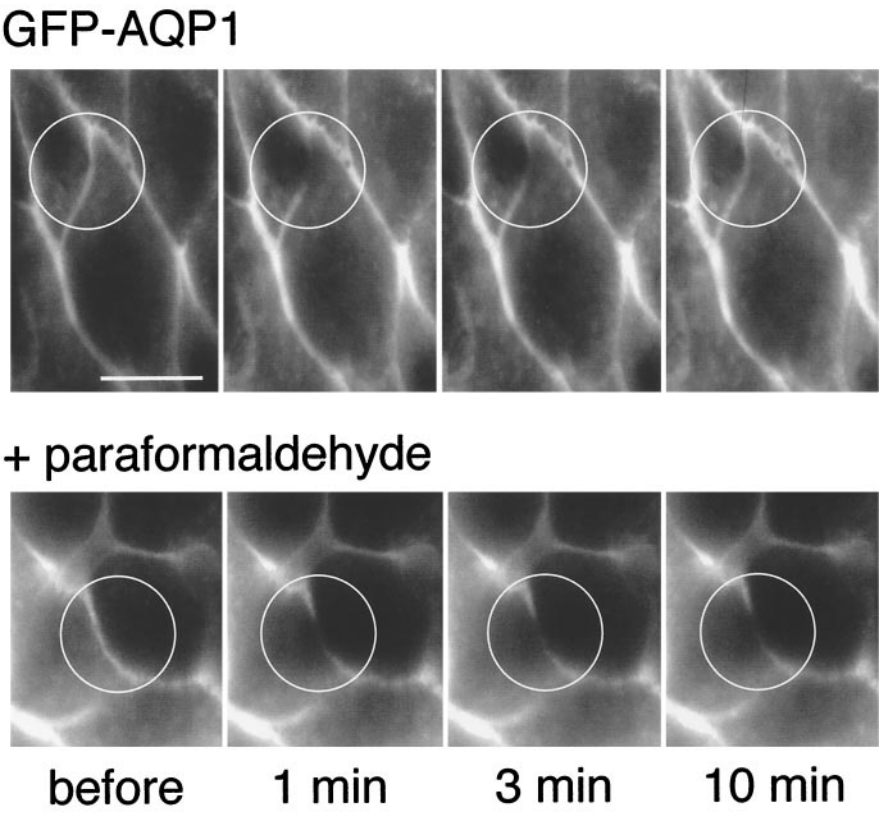

FIGURE 3 Fluorescence recovery after photobleaching of GFP-AQP1-expressing LLC-PK1 cells. Four serial images from a data set are shown. The images displayed were recorded immediately before and 1, 3, and 10 min after a 100-ms photobleaching pulse. The plasma membrane bleach spot is located in the circle. Data are shown for (*top*) control GFP-AQP1-expressing cells and (bottom) after a 60-min incubation with 4% paraformaldehyde in PBS. Scale bar, 10 μm.

from experimental $t_{1/2}$ using an empirical D versus $t_{1/2}$ calibration curve generated from Eq. 1 with $d = 0.8$ μm (Olveczki and Verkman, 1998).

Confocal laser scanning microscopy

Confocal laser scanning microscopy was done on a Zeiss LSM 410 confocal microscope equipped with a Krypton-Argon laser using the 100× objective lens. GFP fluorescence was excited at 488 nm and detected using a 515–565-nm bandpass filter. Cells were grown on glass coverslips and mounted on microscope slides with Vectashield (Vector, Burlingame, CA). Image reconstructions were done with Zeiss LSM or MetaMorph software.

RESULTS

LLC-PK1 cells were stably transfected with GFP-AQP1 or GFP-AQP2, and, for some experiments, MDCK cells were transfected with GFP-AQP2. The GFP-AQP1 and GFP-AQP2 chimeras were evaluated for water transport function and membrane localization. Fig. 1 *A* shows water permeability in *Xenopus* oocytes microinjected with cRNA encoding AQP1, AQP2, and the corresponding GFP-labeled constructs. Osmotically driven water permeability was significantly above that in water-injected oocytes, and the GFP fusion had little effect on aquaporin-mediated water permeability or plasma membrane targeting in oocytes. Fig. 1 *B* shows immunoblot analysis of homogenates from stably transfected LLC-PK1 cells. The fusion proteins had the expected molecular sizes when probed by GFP or aquaporin-specific antibodies. There was no detectable unfused GFP or aquaporin protein. Fig. 1 *C* shows the cellular localization of GFP by laser scanning confocal microscopy (*top*, *xy* sections; *bottom*, *xz* sections). Nearly every clonal population of cells expressing GFP-AQP1 in LLC-PK1 cells showed plasma membrane fluorescence that was greater at the basolateral than the apical membrane (Fig. 1 *C*, *left*). Clonal populations of GFP-AQP2 transfected in LLC-PK1 cells were heterogeneous with some clones showing GFP fluorescence in intracellular vesicles in the absence of cAMP stimulation as reported previously (Gustafson et al., 1998). For the measurements of membrane diffusion below, GFP-AQP2 clones were selected that showed mainly plasma membrane localization both before and after cAMP stimulation (Fig. 1 *C*, *middle*). The GFP fluorescence was seen at the basolateral membrane, in agreement with the

(×430,000). See text for averaged IMP densities. (*B*) Distribution of IMP diameters of control LLC-PK1 cells (*open triangles*), and cells transfected with GFP-AQP1 (*filled circles*) and GFP-AQP2 (*open circles*). Data were fitted to unimodal Gaussian distributions with mean diameters of 5.8 nm (control), 8.0 nm (GFP-AQP1) and 8.2 nm (GFP-AQP2).

findings of Katsura et al. (1995) for AQP2-expressing LLC-PK1 cells. Some experiments were done using a clone of MDCK cells stably expressing GFP-AQP2 (Fig. 1 *C*, *right*) that showed GFP fluorescence in both apical and basolateral plasma membranes.

Membrane ultrastructure of the aquaporin-expressing cells was studied by freeze-fracture electron microscopy. The basolateral plasma membrane of nontransfected LLC-PK1 cells showed relatively low densities of intramembrane particles (IMPs) (Fig. 2 *A*, *panel a*, 2151 ± 352 IMPs/μm^2). IMP densities were significantly greater in cells expressing GFP-AQP1 (*panel b*, 3792 ± 251 IMPs/μm^2) and GFP-AQP2 (*panel c*, 3137 ± 355 IMPs/μm^2). IMP density in the GFP-AQP2-expressing cells after forskolin stimulation was 3231 ± 368 IMPs/μm^2 (*panel d*), indicating that GFP-AQP2 is constitutively present at the cell basolateral plasma membrane in the clonal cell population used here. Apical membrane IMP densities in cells expressing GFP-AQP2 were identical to those in nontransfected cells (1548 ± 142 IMPs/μm^2 versus 1581 ± 172 IMPs/μm^2, respectively) and moderately increased in cells expressing GFP-AQP1 (2096 ± 176 IMPs/μm^2), consistent with the confocal micrographs. In cells expressing aquaporins, numerous larger IMPs were seen, which, at higher magnification, had the characteristic tetrameric appearance of aquaporins (*insets*, *panels b* and *c*) as reported previously (Verbavatz et al., 1993). Figure 2 *B* shows a quantitative analysis of IMP diameters. In control cells, IMP densities were low, and the distribution of IMP greatest diameters fitted a unimodal Gaussian function with mean diameter 5.8 nm. Compared to the nontransfected cells, the GFP-aquaporin-expressing cells had a greater IMP density, The additional populations of IMPs in the transfected cells were observed as unimodal size distributions with mean diameters of 8.0 nm (GFP-AQP1) and 8.2 nm (GFP-AQP2), in agreement with diameters reported for transfected and native cell membranes expressing AQP1 (in the absence of GFP) (Verbavatz et al., 1993; Van Hoek et al., 1995). These results suggest that GFP fusion to the aquaporin N-terminus does not alter the tetrameric association of aquaporins at the plasma membrane.

Figure 3 *A* shows a sequence of fluorescence micrographs of LLC-PK1 cells expressing GFP-AQP1. The leftmost micrograph shows the cell before illumination by a large 5-μm-diameter laser spot. Fluorescence was remarkably reduced in the bleached region after the laser pulse, followed by progressive fluorescence recovery over 10 min to approximately the initial level. In contrast, a similar

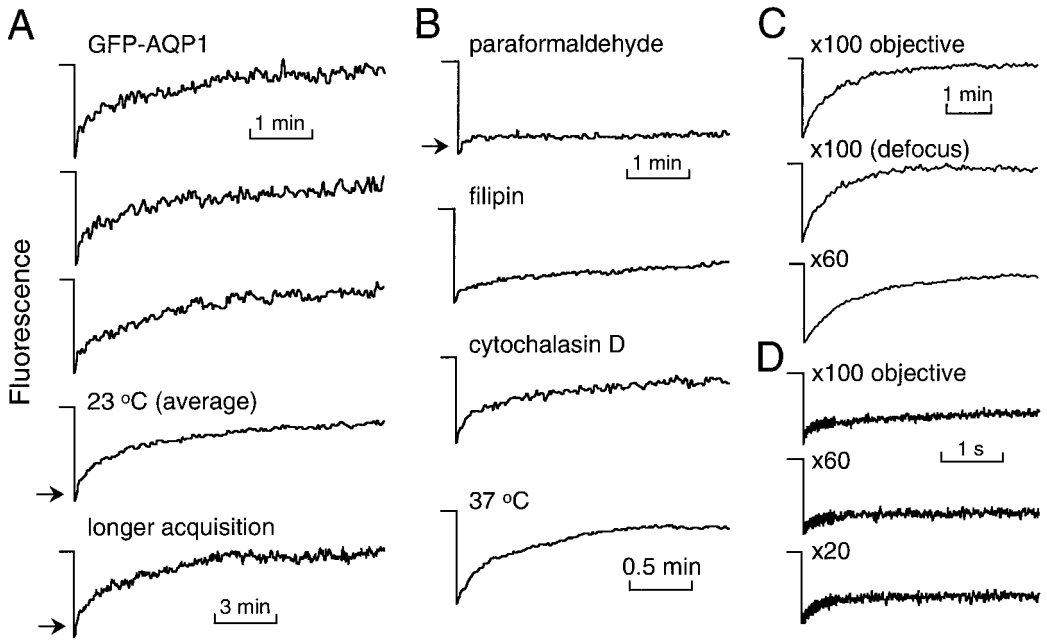

FIGURE 4 Analysis of GFP-AQP1 diffusion in LLC-PK1 cells. The fluorescent cell edge was illuminated with a focused 488-nm laser beam using a 100× oil immersion objective to produce an ~0.8 μm diameter spot. Bleach was accomplished by illumination at high laser intensity for 5 ms. Unless specified, measurements were done at 23°C. (*A*) FRAP measurement of GFP-AQP1 diffusion in transfected LLC-PK1 cells. Shown are three representative individual recovery curves (*top curves*), an averaged recovery curve for 10 different cells (*4th curve*) and an averaged curve for 5 different cells recorded over a longer time. Arrows denote a rapid fluorescence increase arising from reversible (nondiffusion-dependent) photobleaching (see text). (*B*) Same as in *A*, except that cells were treated with paraformaldehyde (4%, 23°C, 1 h), filipin III (10 μM, 23°C, 10 min) or cytochalasin D (5 μg/ml, 37°C, 45 min). Where indicated, FRAP was done on control cells at 37°C. Each curve is the average of 5–15 individual recovery curve from different cells. (*C*) Effect of laser spot size and focus. Spot size was varied from 0.8 and 1.5 μm by using 100× and 60× objective lenses. Where indicated, the spot was defocused by 2 μm above the focal plane. (*D*) FRAP measurement of untreated GFP-AQP1 expressing LLC-PK1 cells showing high time-resolution data using indicated objective lenses. See text for fitted time constants and explanations.

measurement in paraformaldehyde-fixed cells showed no fluorescence recovery over 10 min (Fig. 3 *B*), confirming that the recovery was related to translational GFP-AQP1 diffusion in the plasma membrane.

Quantitative analysis of GFP-AQP1 diffusion was carried out by spot photobleaching in which an 0.8-μm-diameter spot was positioned at the brightly fluorescent cell edge, representing primarily the basolateral plasma membrane. Photobleaching was accomplished by a brief bleach time of 5 ms using an acousto-optic modulator to produce a 20–30% decrease in fluorescence intensity at the end of the bleach time. Fluorescence was then monitored in the same spot using intermittent illumination to avoid bleaching by the probe beam. Figure 4 *A* shows three representative recovery curves from single cells (*top three curves*) and an averaged recovery curve from 10 different cells. At 23°C, fluorescence recovered with a $t_{1/2}$ of 37.5 s, with >92% recovery by 300 s (see Fig. 8 for averaged results). Data recorded over a longer time showed >96% recovery, indicating that nearly all GFP-AQP1 was mobile (Fig. 4 *A*, *bottom curve*). It was consistently found that the recovery curves contained an initial very rapid increase in fluorescence over the first second (*arrows*) (see below). Figure 4 *B* shows that GFP-AQP1 diffusion was abolished (except for the initial rapid fluorescence increase) by paraformaldehyde. GFP-AQP1 diffusion was remarkably slowed by the cholesterol-binding agent filipin, as was reported previously for the membrane diffusion of immunoglobulin E-receptor complexes (Feder et al., 1994). GFP-AQP1 diffusion was not affected by the actin-disrupting agent cytochalasin D. At 37°C, GFP-AQP1 diffusion was increased ~1.6-fold over that at 23°C.

To relate recovery rates to absolute diffusion coefficients (D, in cm^2/s) a mathematical model was used that took into account beam and bleach zone geometry. As described in Methods, the diffusion equation was solved for bleaching of a rectangular region corresponding to bleaching at the cell edge. Computed D values for GFP-AQP1 were 5.3×10^{-11} cm^2/s at 23°C and 9.3×10^{-11} cm^2/s at 37°C.

Several types of measurements were done to justify the quantitative accuracy of diffusion coefficient determination. First, fluorescence recovery was measured in GFP-AQP1-expressing cells at 23°C using a large spot size produced by a 60× objective (1.5-μm-diameter spot) (Fig. 4 *C*). The computed D value was 6.0×10^{-11} cm^2/s, in agreement with that determined for the 100× objective. For experiments in which the bleached spot size was very large (as in Fig. 3 *A*), similar D values in the range $4.2–5.2 \times 10^{-11}$ cm^2/s were found. To determine whether a difference in cell height could affect measured D values, cells were osmotically swelled to double their volume just before photobleaching. There was no effect on recovery time or deduced D value (data not shown). Finally, spot photobleaching measurements were done using the 100× objective in which the spot was defocused by 2 μm above the focus plane (Fig. 4 *C*, *middle curve*). There was <5% change in apparent D

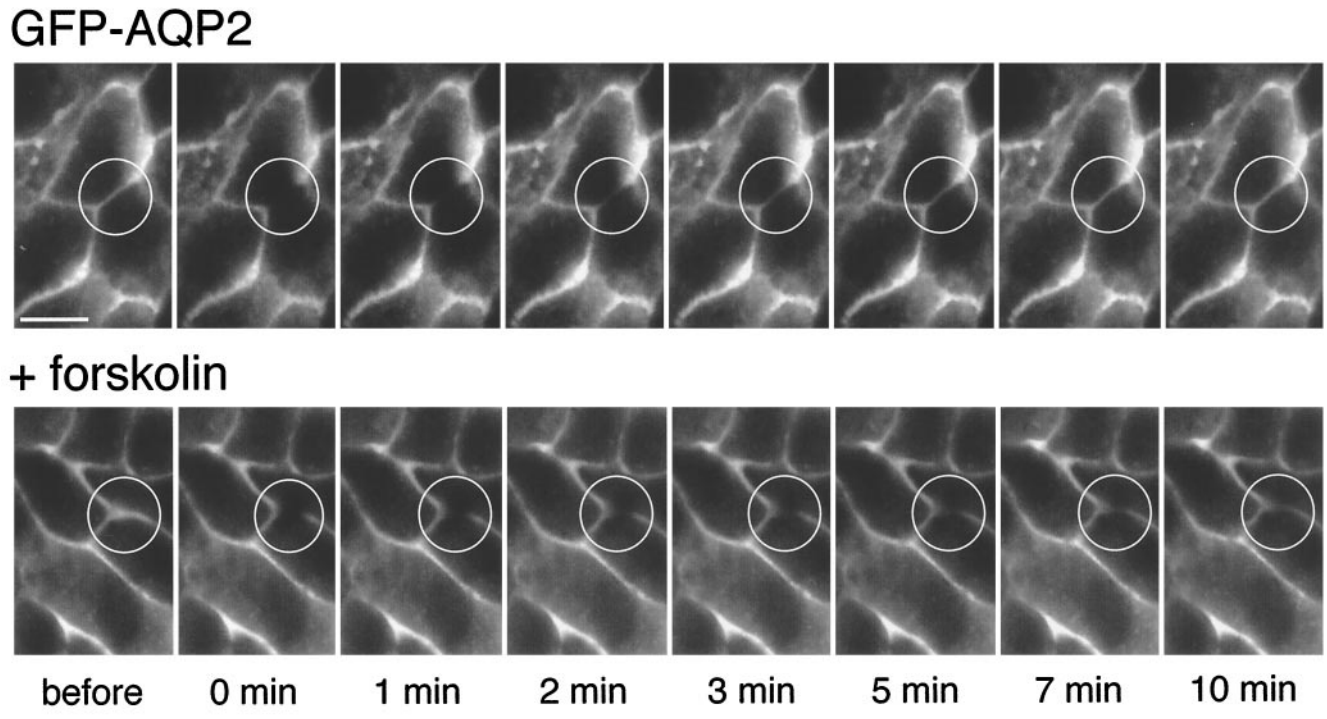

FIGURE 5 Fluorescence photobleaching of GFP-AQP2-expressing LLC-PK1 cells. Sequence of fluorescence micrographs taken before and after photobleaching of a large spot (~5-μm diameter) in (*top*) control cells and (*bottom*) after 15 min incubation with forskolin. Scale bar, 10 μm.

values. These data support the accuracy and robustness of diffusion coefficient determination.

To further characterize the very fast fluorescence recovery process denoted by the arrows, FRAP measurements were done with high temporal resolution using 100×, 60×, and 20× objective lenses (Fig. 4 *D*). The time course of the fast recovery was not affected by beam spot diameter ($t_{1/2}$: 202 ms, 100×; 189 ms, 60×; 196 ms, 20×), indicating that it did not represent GFP-AQP1 diffusion. Together with related evidence (effects of bleach beam intensity and duration, data not shown), it was concluded that the fast process is reversible GFP photobleaching probably involving a triplet state relaxation process. We previously characterized similar fast relaxation processes in studies of fluorescein diffusion in viscous media (Periasamy et al., 1996) and GFP diffusion in cytoplasm (Swaminathan et al., 1997) and endoplasmic reticulum (Dayel et al., 1999). For the measurements here of GFP-aquaporin diffusion in membranes, the reversible photobleaching process was much faster than the diffusion-related recovery. For subsequent presentation and analysis, the first second of recovery data is not shown or included in the analysis.

Photobleaching experiments were next done on LLC-PK1 cells expressing GFP-AQP2 (Fig. 5). In unstimulated cells (Fig. 5, *top*), the fluorescence recovery rate was similar to that of GFP-AQP1. However, incubation with the cell-permeable cAMP agonist forskolin for 15 min clearly reduced the rate of fluorescence recovery (Fig. 5, *bottom*). Figure 6 *A* shows the quantitative spot photobleaching measurements of GFP-AQP2 in unstimulated LLC-PK1 cells. The fluorescence recovered by >98%, as found for GFP-AQP1, with D values of 5.7×10^{-11} cm^2/s at 23°C and 9.0×10^{-11} cm^2/s at 37°C. GFP-AQP2 diffusion was abolished by paraformaldehyde and greatly slowed by filipin, as was found for GFP-AQP1.

Figure 6 *B* shows the slowed membrane diffusion of GFP-AQP2 but not GFP-AQP1 after cAMP stimulation by forskolin. After washout of forskolin, the fluorescence recovery of GFP-AQP2 became rapid, indicating reversible regulation of GFP-AQP2 diffusion by forskolin. Similar forskolin-induced slowing of recovery was found in stably transfected MDCK cells expressing GFP-AQP2 (Fig. 6 *C*).

A series of maneuvers was done to investigate the mechanism by which forskolin treatment resulted in decreased GFP-AQP2 mobility. Representative original recovery curves for spot photobleaching measurements are shown in Fig. 7 and the averaged fitted results are given in Fig. 8. The cell permeable cAMP agonist CPT-cAMP slowed GFP-AQP2 mobility (Fig. 7 *A*), as was found for forskolin, confirming that the slowed diffusion was a cAMP effect. To

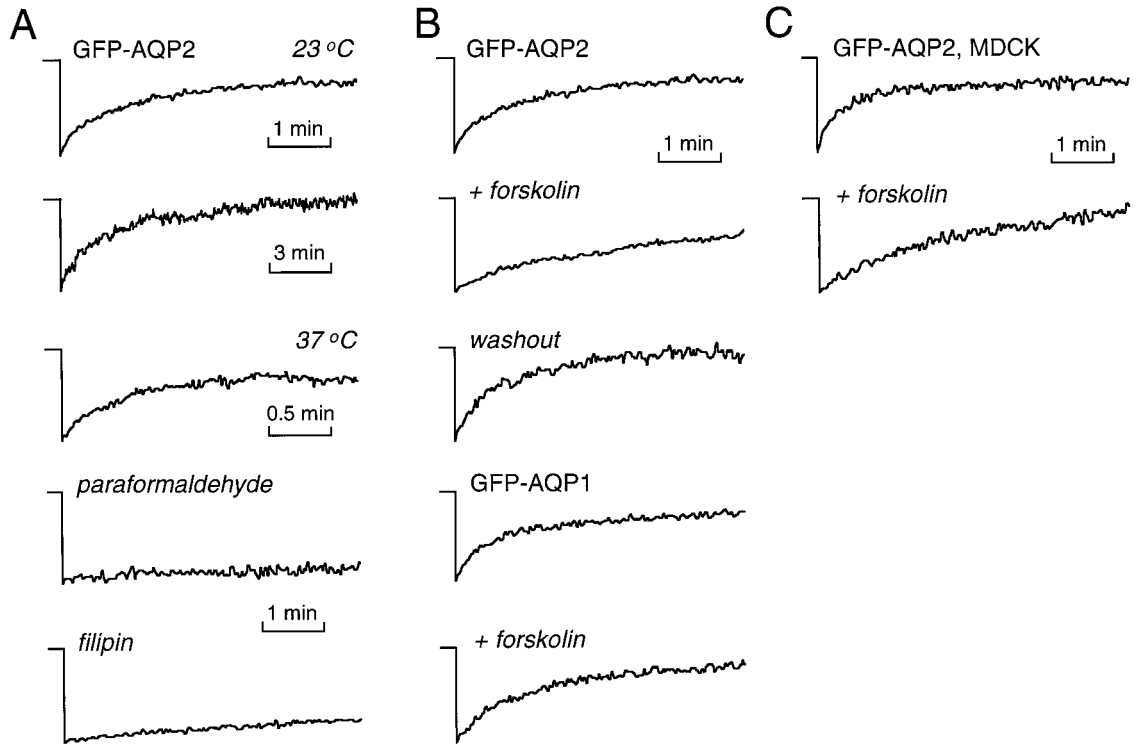

FIGURE 6 (*A*) Analysis of GFP-AQP2 diffusion in LLC-PK1 cells. Experiments were done using various maneuvers as done for GFP-AQP1 diffusion in Fig. 4 *B*. (*B*) Effect of forskolin treatment on GFP-AQP1- and GFP-AQP2-expressing LLC-PK1 cells. Where indicated (+*forskolin*), cells were treated with 50 μM forskolin at 37°C for 15 min, and forskolin was present during FRAP measurements. Where indicated (*washout*), after forskolin stimulation cells were washed with PBS and incubated with PBS for 15 min. (*C*) Measurements as in *B* were done in MDCK cells stably transfected with GFP-AQP2.

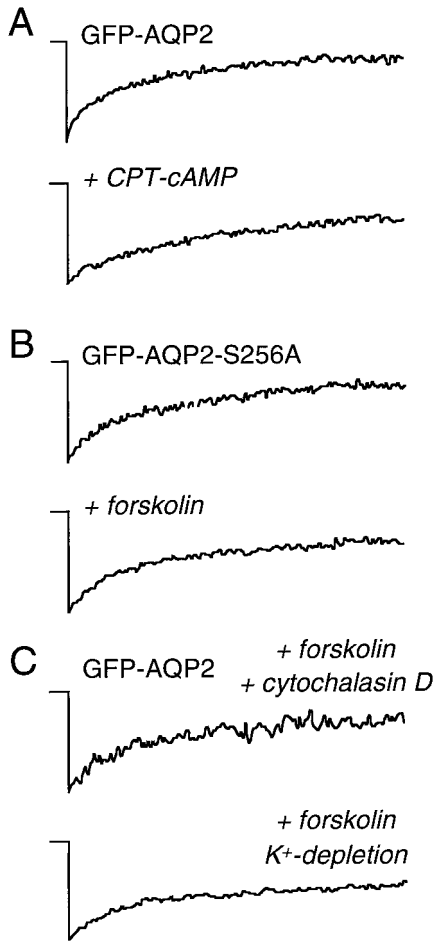

FIGURE 7 Mechanistic analysis of forskolin-regulated GFP-AQP2 diffusion in transfected LLC-PK1 cells. (*A*) FRAP measurements before and after intracellular cAMP stimulation by a 15-min incubation with CPT-cAMP at 37°C. (*B*) Forskolin stimulation studies (as in Fig. 6 *B*) for LLC-PK1 cells stably expressing GFP-S256A-AQP2. (*C*) LLC-PK1 cells expressing wild-type GFP-AQP2 were stimulated with forskolin for 15 min at 37°C, and cytochalasin D (5 μg/ml, 45 min, 37°C) was added in the continued presence of forskolin, or cells were subjected to hypotonic shock in low K^+ medium for 15 min in the continued presence of forskolin.

determine whether phosphorylation at serine 256 was required for the forskolin effect, the mutant S256A was generated, fused with GFP, and expressed in LLC-PK1 cells. Stably transfected clones with a plasma membrane fluorescence pattern were selected as described above. FRAP measurements showed that GFP-AQP2-S256A diffusion was similar to that of the wild-type GFP-AQP2. However, unlike wild-type GFP-AQP2, forskolin treatment did not slow GFP-AQP2-S256A diffusion. Therefore, AQP2 phosphorylation at serine 256 is required for the forskolin-induced slowing of GFP-AQP2 diffusion.

As described in the Introduction, actin filaments and clathrin-mediated endocytosis have been proposed to be involved in AQP2 trafficking. Fig. 7 *C* shows that the actin-disrupting agent cytochalasin D, when added at 15 min after forskolin stimulation (but during continued forskolin presence), reversed the forskolin slowing of wild-type GFP-AQP2 diffusion. As was found for GFP-AQP1, cytochalasin D did not itself affect GFP-AQP2 diffusion in the absence of forskolin (see Fig. 8). Incubation of cells with low K^+/hypotonic medium (during continued forskolin presence), which removes the majority of clathrin from plasma membrane-coated pits (Madshus et al., 1987), resulted in a partial reversal of the forskolin-induced slowing of GFP-AQP2 fluorescence recovery.

Figure 8 summarizes averaged fluorescence recovery rates for spot photobleaching measurements for the various experimental conditions examined in this study. Figure 8 *A* shows that the reciprocal recovery half-times ($1/t_{1/2}$) were similar for GFP-AQP1 and GFP-AQP2 in unstimulated cells, and effects of paraformaldehyde and filipin were similar. Forskolin treatment produced significant slowing of the fluorescence recovery of GFP-AQP2 but not GFP-AQP1. Figure 8 *B* summarizes the effects of the various maneuvers in the GFP-AQP2-expressing cells. Recovery rates are given both as $1/t_{1/2}$ and $1/t_{1/4}$ (reciprocal quarter-times) because sometimes the maneuvers produced subtle differences in recovery curve shapes suggesting biphasic responses. The forskolin effect was reversed by washout and cytochalasin treatment, which, interestingly, resulted in faster recovery than before forskolin treatment. The forskolin effect was partially reversed by the K^+-depletion/hypotonic treatment. The forskolin effect was absent in AQP2-S256A-expressing LLC-PK1 but seen in MDCK cells expressing wild-type GFP-AQP2. A schematic model that incorporates these observations is presented in Fig. 9 and is discussed below.

DISCUSSION

The regulation of collecting-duct water permeability by vasopressin occurs by the endocytosis and exocytosis of AQP2-containing vesicles. Several lines of evidence have suggested that the cytoskeleton plays an important role in this mechanism (reviewed in Brown and Stow, 1996; Brown et al., 1998). The vasopressin-dependent increase in water permeability is impaired by disruption of microtubules or microfilaments both in amphibian urinary bladder and kidney collecting duct (Franki et al., 1992; Simon et al., 1993; Marples et al., 1996). Preliminary evidence in collecting-duct principal cells suggests that AQP2 phosphorylation occurs in intracellular vesicles before exocytosis (Christensen et al., 1998). Finally, colocalization studies suggest that the plasma membrane targeting of AQP2-containing vesicles to the plasma membrane might involve VAMP-2 (Nielsen et al., 1995b), syntaxin-4 (Mandon et al., 1996), and Rab3a and heterotrimeric G proteins (Valenti et al., 1998). However, there has been no direct evidence for an in vivo interaction between phosphorylated AQP2 and any other protein.

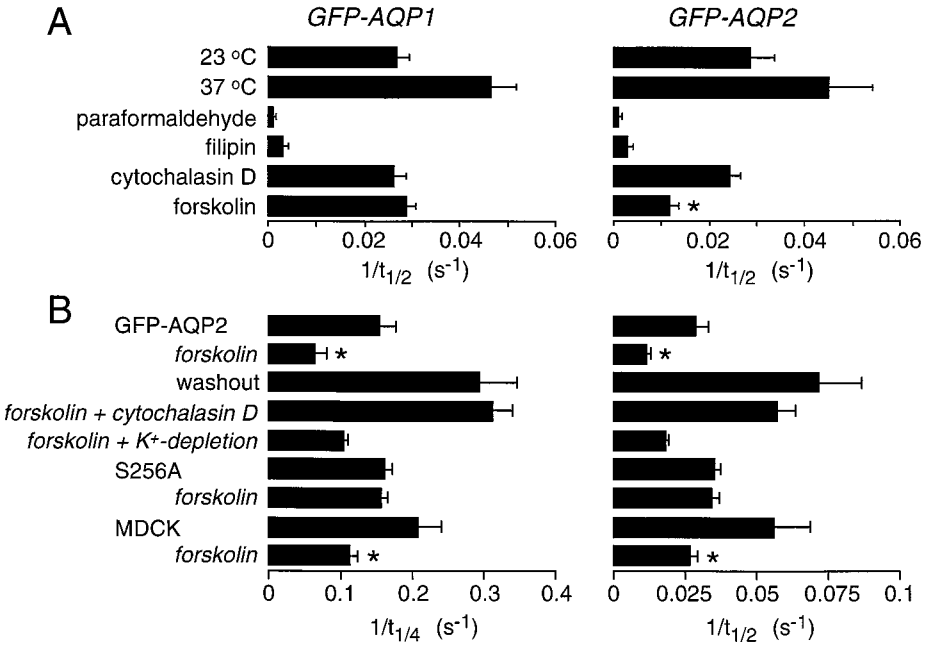

FIGURE 8 Summary of spot photobleaching experiments. Data shown as reciprocal half-times ($t_{1/2}$) or quarter-times ($t_{1/4}$) for fluorescence recovery (mean ± SE, $n = 4–10$ separate sets of measurements). Maneuvers correspond to those given in Figs. 4, 6 and 7. * $p < 0.001$ compared to control (without forskolin).

We report here that the mobility of wild-type AQP2 in plasma membranes was reduced after forskolin addition, whereas the mobility of AQP1 was unaffected. The replacement of serine 256 of AQP2 with alanine resulted in the loss of forskolin sensitivity, providing evidence for a direct interaction between phosphorylated AQP2 with other membrane protein(s) or cytoskeletal elements during vasopressin stimulation. The cytochalasin D reversal of the forskolin-induced decrease in AQP2 mobility suggested a functionally significant interaction between AQP2 and actin microfilaments by direct or indirect interactions. Immunogold electron microscopy of rat kidney has shown abundant AQP2 localization in actin-rich apical plasma membrane microvilli during vasopressin stimulation (Nielsen et al., 1995a; Yamamoto et al., 1995). AQP2 internalization is believed to occur by endocytosis of clathrin-coated vesicles from plasma membrane-coated pits (Strange et al., 1988; Katsura et al., 1995). We found that K^+-depletion/hypotonic shock, established maneuvers to inhibit clathrin-mediated endocytosis (Hansen et al., 1993), partially blocked the decrease in AQP2 mobility in response to forskolin. Together, these observation suggest that AQP2 phosphorylation during vasopressin challenge is associated with AQP2 interactions with the cytoskeleton and coated pits involved in both exocytosis and endocytosis. We postulate that these interactions play a role in the vasopressin-stimulated recycling of AQP2 water channels in kidney collecting-duct principal cells.

The diffusion of the GFP-aquaporin chimeras in unstimulated cells was unrestricted and had diffusion coefficients of $5–9 \times 10^{-11}$ cm^2/s. Recently, GFP has been used to tag a few membrane proteins for diffusion measurements. The lateral diffusion coefficient of GFP-Ki-Ras expressed at plasma membrane in Rat-1 cells was 1.9×10^{-9} cm^2/s with a high mobile fraction of 94% (Niv et al., 1999). Similar diffusion was found for a gonadotropin-releasing hormone receptor-GFP chimera in CHO cells ($1.2–1.6 \times 10^{-9}$ cm^2/s, mobile fraction 76–91%) (Nelson et al., 1999). The diffu-

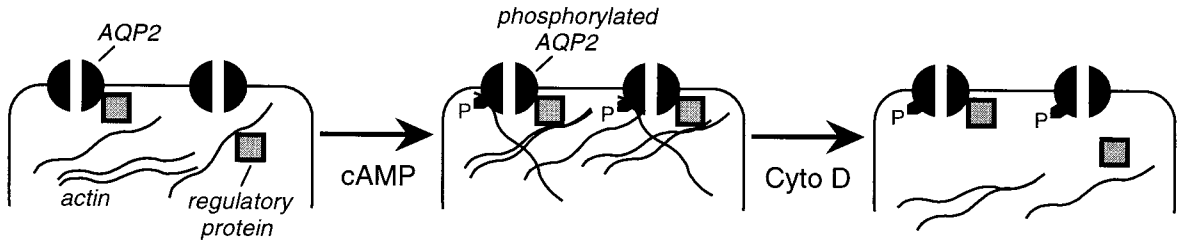

FIGURE 9 Model for GFP-AQP2 diffusion in epithelial cell plasma membranes. In the basal state, AQP2 is depicted at the plasma membrane with little or no interactions with regulatory or skeletal proteins. After cAMP stimulation, AQP2 and possibly various regulatory protein(s) become phosphorylated, resulting in AQP2–protein interactions and a corresponding decrease in AQP2 lateral mobility in the plane of the membrane. Cytochalasin D treatment disrupts actin interactions and permits unhindered AQP2 mobility. See text for further explanations.

sion coefficient of β_2-adrenergic receptor-GFP expressed at the plasma membrane in HEK 293 cells was higher ($4–12 \times 10^{-9}$ cm^2/s, mobile fraction 75 ± 20%) (Barak et al., 1997). These values are somewhat greater than the diffusion coefficients measured here for GFP-AQP1 and GFP-AQP2. The tetrameric association and considerable hydrophobicity of the integral membrane aquaporin proteins probably contributes to their low membrane diffusion. Cho et al. (1999) reported a FRAP measurement of AQP1 diffusion in intact erythrocytes, in which membrane AQP1 was fluorescently labeled by anti-AQP1 antibody. At 37°C, the diffusion coefficient was 3.1×10^{-11} cm^2/s with a mobile fraction of 66 ± 10%. The low AQP1 diffusion coefficient in erythrocytes may be related to the presence of the spectrin membrane skeleton or to interactions of the externally added antibody with the erythrocyte glycocalyx. Further biochemical studies are needed to investigate these possibilities.

A pictorial model summarizing the data for GFP-AQP2 is given in Fig. 9. Before cAMP stimulation, unphosphorylated AQP2 is shown as interacting little with skeletal or other proteins, and thus relatively mobile in the plane of the membrane. After phosphorylation, AQP2 translocates specialized membrane patches, such as clathrin-coated pits, in which association with actin and/or other membrane proteins occurs. The lateral mobility of actin-associated, phosphorylated AQP2 is much lower than that of nonphosphorylated AQP2 in its basal state. After actin filament disruption, AQP2 mobility again becomes high. Interestingly, the lateral mobility of AQP2 after cytochalasin was greater than that before forskolin stimulation, possibly because of AQP2 accumulation in a more fluid membrane patch during cAMP stimulation or because of weak actin–AQP2 interactions before forskolin treatment. The cAMP-dependent slowed AQP2 mobility and retention in specialized membrane domains may be important for efficient AQP2 endocytic retrieval. Our results thus provide direct biophysical evidence for interaction of plasma membrane AQP2 with one or more regulatory proteins. The challenge will be to identify these proteins.

We thank N. Periasamy and Mark Dayel for assistance in modifying the FRAP apparatus, and Gavin Thurston for assistance in laser confocal scanning microscopy.

This work was supported by grants DK35124, DK43840, HL59198 and HL60288 from the National Institutes of Health.

REFERENCES

Bai, C. X., N. Fukuda, Y. Song, T. Ma, M. A. Matthay, and A. S. Verkman. 1999. Lung fluid transport in aquaporin-1 and aquaporin-4 knockout mice. *J. Clin. Invest.* 103:555–561.

Barak, L. S., S. G. Ferguson, J. Zhang, C. Martenson, T. Meyer, and M. G. Caron. 1997. Internal trafficking and surface mobility of a functionally intact β_2-adrenergic receptor-green fluorescent protein conjugate. *Mol. Pharmacol.* 51:177–184.

Bichet, D. G. 1998. Nephrogenic diabetes insipidus. *Am. J. Med.* 47: 1344–1347.

Brown, D., C. Cunningham, J. Hartwig, M. McLaughlin, and T. Katsura. 1996. Association of AQP2 with actin in transfected LLC-PK1 cells and rat papilla. *J. Am. Soc. Nephrol.* 7:1265 (abstract).

Brown, D., and J. L. Stow. 1996. Protein trafficking and polarity in kidney epithelium: from cell biology to physiology. *Physiol. Rev.* 76:245–297.

Brown, D., T. Katsura, and C. E. Gustafson. 1998. Cellular mechanisms of aquaporin trafficking. *Am. J. Physiol.* 275:F328–F331.

Cheng, A., A. N. van Hoek, M. Yeager, A. S. Verkman, and A. K. Mitra. 1997. Three-dimensional organization of a human water channel. *Nature.* 387:627–630.

Cho, M. R., D. W. Knowles, B. L. Smith, J. J. Moulds, P. Agre, N. Mohandas, and D. E. Golan. 1999. Membrane dynamics of the water transport protein aquaporin-1 in intact human red cells. *Biophys. J.* 76:1136–1144.

Christensen, B. M., M. Zelenina, A. Aperia, and S. Nielsen. 1998. Localization of phosphorylated aquaporin-2 in kidney collecting duct principal cells in response to dDAVP or V2-receptor antagonist treatment. *J. Am. Soc. Nephrol.* 9:16A (abstract).

Dayel, M., E. Hom, and A. S. Verkman. 1999. Diffusion of green fluorescent protein in the aqueous lumen of endoplasmic reticulum. *Biophys. J.* 76:2843–2851.

Deen, P. M. T., M. A. Verkijk, N. V. Knoers, B. Wieringa, L. A. Monnens, C. H. van Os, and B. A. Van Oost. 1994. Requirement of human renal water channel aquaporin-2 for vasopressin-dependent concentration of urine. *Science.* 264:92–95.

Deen, P. M. T., H. Croes, R. A. van Aubel, L. A. Ginsel, and C. H. van Os. 1995. Water channels encoded by mutant aquaporin-2 genes in nephrogenic diabetes insipidus are impaired in their cellular routing. *J. Clin. Invest.* 95:2291–2296.

Deen, P. M. T., J. P. Rijss, S. M. Mulders, R. J. Errington, J. van Baal, and C. H. van Os. 1997. Aquaporin-2 transfection of Madin–Darby canine kidney cells reconstitutes vasopressin-regulated transcellular osmotic water transport. *J. Am. Soc. Nephrol.* 8:1493–1501.

Deen, P. M. T., and C. H. van Os. 1998. Epithelial aquaporins. *Curr. Opin. Cell Biol.* 10:435–442.

Feder, T. J., E. Chang, D. Holowka, and W. W. Webb. 1994. Disparate modulation of plasma membrane protein lateral mobility by various cell permeabilizing agents. *J. Cell. Physiol.* 158:7–16.

Franki, N., G. Ding, Y. Gao, and R. M. Hays. 1992. Effect of cytochalasin D on the actin cytoskeleton of the toad bladder epithelial cell. *Am. J. Physiol.* 263:C95–C100.

Fushimi, K., S. Sasaki, and F. Marumo. 1997. Phosphorylation of serine 256 is required for cAMP-dependent regulatory exocytosis of the aquaporin-2 water channel. *J. Biol. Chem.* 272:14800–14804.

Gustafson, C. E., S. Levine, T. Katsura, M. McLaughlin, M. D. Aleixo, B. K. Tamarappoo, A. S. Verkman, and D. Brown. 1998. Vasopressin regulated trafficking of a green fluorescent protein-aquaporin 2 chimera in LLC-PK1 cells. *Histo. Cell Biol.* 110:377–386.

Hansen, S. H., K. Sandvig, and B. van Deurs. 1993. Molecules internalized by clathrin-independent endocytosis are delivered to endosomes containing transferrin receptors. *J. Cell Biol.* 123:89–97.

Inoue, T., S. Nielsen, B. Mandon, J. Terris, B. K. Kirshore, and M. A. Knepper. 1998. SNAP-23 in rat kidney: colocalization with aquaporin-2 in collecting duct vesicles. *Am. J. Physiol.* 275:F752–F760.

James, D. E., R. C. Piper, and J. W. Slot. 1994. Insulin stimulation of GLUT-4 translocation: a model for regulated recycling. *Trends Cell Biol.* 4:120–125.

Kao, H. P., and A. S. Verkman. 1996. Construction and performance of a FRAP instrument with microsecond time resolution. *Biophys. Chem.* 59:203–210.

Katsura, T., J. M. Verbavatz, J. Farinas, T. Ma, D. A. Ausiello, A. S. Verkman, and D. Brown. 1995. Constitutive and regulated membrane expression of aquaporin-CHIP and aquaporin-2 water channels in stably transfected LLC-PK1 cells. *Proc. Natl. Acad. Sci. USA.* 92:7212–7216.

Katsura, T., C. E. Gustafson, D. A. Ausiello, and D. Brown. 1997. Protein kinase A phosphorylation is involved in regulated exocytosis of aquaporin-2 in transfected LLC-PK1 cells. *Am. J. Physiol.* 272:F817–F822.

Knepper, M. A., and T. Inuoe. 1997. Regulation of aquaporin-2 water channel trafficking by vasopressin. *Curr. Opin. Cell Biol.* 9:560–564.

Kornau, H. C., P. H. Seeburg, and M. B. Kennedy. 1997. Interaction of ion channels and receptors with PDZ domain proteins. *Curr. Opin. Neurobiol.* 7:368–373.

Lee, M. D., L. S. King, and P. Agre. 1997. The aquaporin family of water channel proteins in clinical medicine. *Medicine (Baltimore).* 76: 141–156.

Lencer, W. I., A. S. Verkman, D. A. Ausiello, A. Arnaout, and D. Brown. 1990. Endocytic vesicles from renal papilla which retrieve the vasopressin-sensitive water channel do not contain an H^+ ATPase. *J. Cell Biol.* 111:379–389.

Ma, T., B. Yang, A. Gillespie, E. J. Carlson, C. J. Epstein, and A. S. Verkman. 1998. Severly impaired urinary concentrating ability in transgenic mice lacking aquaporin-1 water channels. *J. Biol. Chem.* 273: 4296–4299.

Madshus, I. H., K. Sandvig, S. Olsnes, and B. van Deurs. 1987. Effect of reduced endocytosis induced by hypotonic shock and potassium depletion on the infection of Hep 2 cells by picornaviruses. *J. Cell Physiol.* 131:14–22.

Mandon, B., C. L. Chou, S. Nielsen, and M. A. Knepper. 1996. Syntaxin-4 is localized to the apical plasma membrane of rat renal collecting duct cells: possible role in aquaporin-2 trafficking. *J. Clin. Invest.* 98: 906–913.

Marples, D., B. Barber, and A. Taylor. 1996. Effect of dynein inhibitor on vasopressin action in toad urinary bladder. *J. Physiol. (London).* 490: 767–774.

Marples, D., T. A. Schroer, N. Ahrens, A. Taylor, M. A. Knepper, and S. Nielsen. 1998. Dynein and dynactin colocalize with AQP2 water channels in intracellular vesicles from kidney collecting duct. *Am. J. Physiol.* 274:F384–F394.

Nelson, S., R. D. Horvat, J. Malvey, D. A. Roess, B. G. Barisas, and C. M. Clay. 1999. Characterization of an intrinsically fluorescent gonadotropin-relasing hormone receptor and effects of ligand binding on receptor lateral diffusion. *Endocrinology.* 140:950–957.

Nielsen, S., C. L. Chou, D. Marples, E. I. Christensen, B. K. Kishore, and M. A. Knepper. 1995a. Vasopressin increases water permeability of kidney collecting duct by inducting translocation of aquaporin-CD water channels to plasma membrane. *Proc. Natl. Acad. Sci. USA.* 92: 1013–1017.

Nielsen, S., D. Marples, H. Birn, M. Mohtashami, N. O. Dalby, M. Trimble, and M. A. Knepper. 1995b. Expression of VAMP-2 like protein in kidney collecting duct intracellular vesicles. Colocalization with aquaporin-2 water channels. *J. Clin. Invest.* 96:1834–1844.

Nielsen, S., T. H. Kwon, B. M. Christensen, D. Promeneur, J. Frokiaer, and D. Marples. 1999. Physiology and pathophysiology of renal aquaporin. *J. Am. Soc. Nephrol.* 10:647–663.

Niv, H., O. Gutman, Y. I. Henis, and Y. Kloog. 1999. Membrane interactions of a constitutively active GFP-Ki-Ras 4B and their role in signaling. *J. Biol. Chem.* 274:1606–1613.

Olveczky, B. P., and A. S. Verkman. 1998. Monte-Carlo analysis of obstructed diffusion in 3 dimensions: application to molecular diffusion in organelles. *Biophys. J.* 74:2722–2730.

Partikian, A., B. P. Olveczky, R. Swaminathan, Y. Li, and A. S. Verkman. 1998. Rapid diffusion of green fluorescent protein in the mitochondrial matrix. *J. Cell Biol.* 140:821–829.

Periasamy, N., S. Bicknese, and A. S. Verkman. 1996. Reversible photobleaching of fluorescein conjugates in air-saturated viscous solution: molecular tryptophan as a triplet state quencher. *Photochem. Photobiol.* 63:265–271.

Shi, B. L., W. Skach, and A. S. Verkman. 1994. Functional independence of monomeric CHIP28 water channels revealed by expression of wild type-mutant heterodimers. *J. Biol. Chem.* 269:10417–10422.

Simon, H., Y. Gao, N. Franki, and R. M. Hays. 1993. Vasopressin depolymerizes apical F-actin in rat inner medulary collecting duct. *Am. J. Physiol.* 265:C757–C762.

Smith, B. L., and Agre, P. 1991. Erythrocyte M_r 28,000 transmembrane protein exists as a multi-subunit oligomer similar to channel proteins. *J. Biol. Chem.* 266:6407–6415.

Strange, K., M. C. Willingham, J. S. Handler, and H. W. Harris. 1988. Apical membrane endocytosis via coated pits is stimulated by removal of antidiuretic hormone from isolated, perfused rabbit cortical collecting ducts. *J. Membr. Biol.* 103:17–28.

Swaminathan, R., N. Periasamy, S. Bicknese, and A. S. Verkman. 1996. Cytoplasmic viscosity near the cell plasma membrane: translation of BCECF measured by total internal reflection-fluorescence photobleaching recovery. *Biophys. J.* 71:1140–1151.

Swaminathan, R., C. P. Hoang, and A. S. Verkman. 1997. Photobleaching properties of green fluorescent protein GFP-S65T in solution and transfected CHO cells: analysis of cytoplasmic viscosity by GFP translational and rotational diffusion. *Biophys. J.* 72:1099–1907.

Tamarappoo, B. K., and A. S. Verkman. 1998. Defective trafficking of AQP2 water channels in nephrogenic diabetes insipidus and correction by chemical chaperones. *J. Clin. Invest.* 101:2257–2267.

Tamarappoo, B. K., B. Yang, and A. S. Verkman. 1999. Misfolding of mutant aquaporin-2 water channels in nephrogenic diabetes insipidus. *J. Biol. Chem.* 274:34825–34831.

Umenishi, F., and A. S. Verkman. 1998. Isolation of the human aquaporin-1 promoter and functional characterization in human erythroleukemia cell lines. *Genomics.* 47:341–349.

Valenti, G., A. Frigeri, P. M. Roncho, C. D'Ettorre, and M. Svelto. 1996. Expression and functional analysis of water channels in a stably AQP2-transfected human collecting duct cell line. *J. Biol. Chem.* 271: 24365–24370.

Valenti, G., G. Procino, U. Liebenhoff, A. Frigeri, P. A. Benedetti, G. Ahnert-Hilger, B. Nurnberg, M. Svelto, and W. Rosenthal. 1998. A heterotrimeric G protein of the Gi family is required for cAMP-triggered trafficking of aquaporin 2 in kidney epithelial cells. *J. Biol. Chem.* 273:22627–22634.

Van Hoek, A. N., M. C. Wiener, J. M. Verbavatz, D. Brown, R. R. Townsend, and A. S. Verkman. 1995. Purification and structure–function analysis of deglycosylated CHIP28 water channels. *Biochemistry.* 34:2212–2219.

Verbavatz, J. M., D. Brown, I. Sabolic, G. Valenti, D. A. Ausiello, A. N. van Hoek, T. Ma, and A. S. Verkman. 1993. Tetrameric assembly of CHIP28 water channels in liposomes and cell membranes. *A* freeze-fracture study. *J. Cell Biol.* 123:605–618.

Verbavatz, J. M, T. Ma, R. Gobin, and A. S. Verkman. 1997. Absence of orthogonal arrays in kidney, brain and muscle from transgenic knockout mice lacking water channel aquaporin-4. *J. Cell Sci.* 110:2855–2860.

Verkman, A. S., W. Lencer, D. Brown, and D. A. Ausiello. 1988. Endosomes from kidney collecting tubule contain the vasopressin-sensitive water channel. *Nature.* 333:268–269.

Verkman, A. S., A. N. van Hoek, T. Ma, A. Frigeri, W. R. Skach, A. Mitra, B. K. Tamarappoo, and J. Farinas. 1996. Water transport across mammalian cell membranes. *Am. J. Physiol.* 270:C12–C30.

Walz, T., T. Hirai, K. Murata, J. B. Heymann, K. Mitsuoka, Y. Fujiyoshi, B. L. Smith, P. Agre, and A. Engel. 1997. The three-dimensional structure of aquaporin-1. *Nature.* 387:624–627.

Yamamoto, T., S. Sasaki, K. Fushimi, K. Ishibashi, E. Yaoita, K. Kawasaki, F. Marumo, and I. Kihara. 1995. Vasopressin increases AQP-CD water channel in apical membrane of collecting duct cells in Brattleboro rats. *Am. J. Physiol.* 268:C1546–C1551.

Yamamoto, T., and S. Sasaki. 1998. Aquaporins in the kidney: emerging new aspects. *Kid. Internat.* 54:1041–1051.

Zhang, R., W. Skach, H. Hasegawa, A. N. van Hoek, and A. S. Verkman. 1993. Cloning, functional analysis and cell localization of a kidney proximal tubule water transporter homologous to CHIP28. *J. Cell Biol.* 120:359–369.